

Broad-frequency dielectric behaviors in multiwalled carbon nanotube/rubber nanocomposites

Mei-Juan Jiang,^{1,2} Zhi-Min Dang,^{1,a)} Michael Bozlar,^{2,3} Fabien Miomandre,³ and Jinbo Bai^{2,b)}

¹Key Laboratory of Beijing City for Preparation and Processing of Novel Polymer Materials, Beijing University of Chemical Technology, Beijing 100029, China

²Laboratoire de Mécanique des Sols, Structures et Matériaux, Ecole Centrale Paris, CNRS UMR8579, PRES UniverSud, Grande Voie des Vignes, 92295 Châtenay-Malabry Cedex, France

³Laboratoire de Photophysique, Photochimie, Supramoléculaires et Macromoléculaires, Ecole Normale Supérieure de Cachan, CNRS UMR8531, PRES UniverSud, 61 Avenue du Président Wilson, 94235 Cachan Cedex, France

(Received 8 May 2009; accepted 6 September 2009; published online 20 October 2009)

Broad-frequency dielectric behaviors of multiwalled carbon nanotubes (MWCNTs) embedded in room temperature vulcanization silicone rubber (RT-SR) matrix were studied by analyzing alternating current (ac) impedance spectra, which would make a remarkable contribution for understanding some fundamental electrical properties in the MWCNT/RT-SR nanocomposites. Equivalent circuits of the MWCNT/RT-SR nanocomposites were built, and the law of polarization and mechanism of electric conductance under the ac field were acquired. Two parallel RC circuits in series are the equivalent circuits of the MWCNT/RT-SR composites. At different frequency ranges, dielectric parameters including conductivity, dielectric permittivity, dielectric loss, impedance phase, and magnitude present different behaviors. © 2009 American Institute of Physics. [doi:10.1063/1.3238306]

I. INTRODUCTION

Electroactive polymer materials are of great interest for a broad range of applications as they exhibit excellent electro-mechanical properties, high electrical conductivity, and high dielectric permittivity far above those of traditional polymers.^{1–4} For these electroactive polymer materials, the most important characteristics include electric polarization and electric conductance, which can bring out a crucial effect on the final dielectric properties.^{4–7} There are mainly two kinds of dielectric polarization systems, one is the dipole system and the other is the charge carrier systems. Meanwhile, a wide range of relaxation phenomena is associated with interfacial phases in metal-insulator, semiconductor-insulator, electrode-electrolyte, and similar systems.^{8–10} For the electrical conductive particle-filled polymer composites, the polarization mechanism is very complex and there is no detailed interpretation until now, especially for the one-dimensional nanofiller/polymer composite systems.

The mechanism of electric conductance of the polymer composites under alternating current (ac) field is still uncertain.^{11,12} There is no exact interpretation about the regulation that the conductivity changes with frequency. One of the most interesting models for ac conductivity (σ_{ac}) in disordered solids is the random free-energy barrier model, which is also referred to as the symmetric hopping model, proposed by Dyre and co-worker.^{13,14} This model is based on the ascertainment that the conductivity is thermally activated, $\sigma(T) \propto \exp(-\Delta E/T)$, where $\sigma(T)$, ΔE , and T are the

electric conductivity, activation energy, and temperature, respectively, and the ac conductivity is less temperature dependent. It suggests that the ac conductivity is dominated by processes with activation energies (ΔE_{ac}) smaller than the direct current (dc) ones ΔE_{dc} . By employing the continuous time random walk approximation and the assumption of a distribution of energy barriers over which only jumps to the nearest-neighbor sites with equal probability are allowed. Dyre derived the ac conductivity in disordered solids as $\sigma_{ac}(\omega) = \sigma_{dc} [j\omega\tau / \ln(1 + j\omega\tau)]$,¹³ where σ_{dc} , ω , and τ are the direct current conductivity, the angular frequency, and the relaxation time, respectively. The random free-energy barrier model has been found to be in agreement with experimental data for a large number of disordered solids.¹⁴

It is well known that the σ_{ac} is the sum of all dissipative effects including an actual Ohmic conductivity caused by migrating charge carriers as well as a frequency-dependent dielectric dispersion.¹⁵ If the random free-energy barrier model is effective, there will be large conduction loss at high frequency, which disagrees with the experimental phenomena. In addition, the dielectric properties of the disorder solid materials can also be described by its equivalent circuits which is composed of resistor (R), capacitor (C), and inductor (L) elements. The total impedance of materials can be composed of resistance and reactance, but not be added together simply. Driven by an ac supply, a capacitor will only accumulate a limited amount of charge before the potential difference is changed. Therefore, if the equivalent circuit of the composites is known, we can understand the polarization mechanism and the ac conduction mechanism according to the basic composition elements of the composites. Just recently, one-dimensional carbon nanotubes (CNTs) with high

^{a)} Author to whom correspondence should be addressed. Electronic mail: dangzm@mail.buct.edu.cn.

^{b)} Electronic mail: jinbo.bai@ecp.fr.

conductivity and unique nanostructure are embedded into polymer matrix to form the disorder composites. Moreover, high conductivity, high dielectric permittivity, and excellent electrostriction in these composites are discovered.^{3,16} However, it is often difficult to explain most of the complex dielectric properties in these disordered composites. Theoretical predictions of the fundamental physical data suffer from a lack of experimental data, especially dielectric data over a wide frequency range.

We therefore conducted high resolution measurements of frequency-dependent dielectric behaviors in the CNT/polymer composites. Room temperature vulcanization silicone rubber (RT-SR) was chosen as polymer matrix because it exhibited a low glassy temperature and a simple preparation process. The results show that two parallel RC circuits in series are the equivalent circuits of the multiwalled CNT (MWCNT)/RT-SR composites. At different frequency ranges, dielectric parameters including conductivity, dielectric permittivity, dielectric loss, impedance phase, and magnitude display different behaviors, respectively. The equivalent circuits of MWCNT/RT-SR nanocomposites were built, and the law of polarization and the mechanism of electric conductance under the ac field were acquired.

II. EXPERIMENTAL PROCEDURES

Raw MWCNTs as received are about 10–30 nm in diameter and 10–15 μm in length. Prior to use, they were chemically modified in ethanol by means of a coupling agent, γ -aminopropyltriethoxy silane in order to improve the affinity between MWCNT fillers and RT-SR matrix. The ethanol solutions with MWCNT powder and the coupling agent were mixed and ultrasonicated for 30 min at RT. After filtration, the modified nanotubes were dried at 100 $^{\circ}\text{C}$ for 24 h. After that, the modified multiwalled nanotubes were achieved. The MWCNT/RT-SR nanocomposites with different volume fractions of CNTs were prepared by three roll mills. First, MWCNT and RT-SR were mixed together manually. The suspension was added batchwise to the three roll miller for final high shear mixing. The gap size between the rollers was 15 μm . The dwell time of each batch of suspension was ≈ 1 min at the speed of 300 rpm and 1 min at 600 rpm, respectively. The suspension was collected, mixing with the hardener for 2 min by hand, cured for 24 h at RT.

The impedance magnitude and the impedance phase of the MWCNT/RT-SR composites were measured by using an impedance analyzer (Solarton 1260), and the real and imaginary parts of the impedance were calculated according to $Z' = |Z|\cos(\theta)$ and $Z'' = |Z|\sin(\theta)$, respectively. The equivalent circuits resulting from the analysis of the impedance spectra were built, and the mechanism of the dielectric relaxation and the electric conductance were explored.

III. RESULTS AND DISCUSSIONS

Figure 1 shows dependences of impedance phase and impedance magnitude of the MWCNT/RT-SR composites on frequency at RT. It is found that the impedance phases are close to 0 and the impedance magnitudes are independent of frequencies below approximately 10 Hz. This suggests that

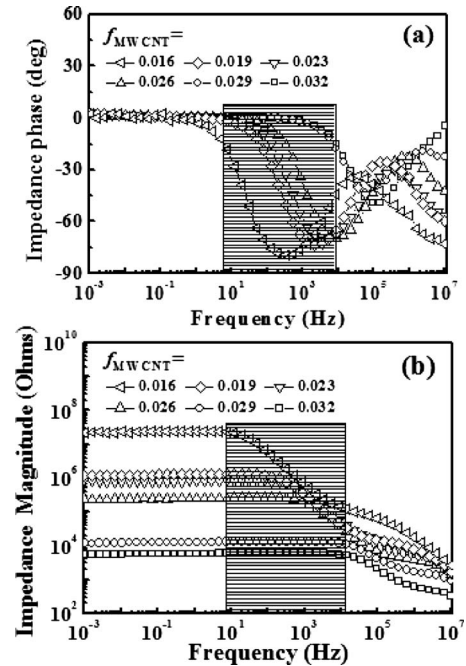


FIG. 1. Dependences of (a) impedance phase and (b) impedance magnitude of the MWCNT/RT-SR composites with different f_{MWCNT} on frequency at RT.

the Ohmic resistance elements play an important role at low frequencies. With increasing frequency further, all of the impedance phases [see Fig. 1(a)] and the impedance magnitudes [see Fig. 1(b)] decrease at the same time, which illustrates the character of capacitor impedance. In the meantime, the peak of impedance phase appears in Fig. 1(a), it is caused by the dielectric relaxation of the MWCNT/RT-SR composites. We also notice that the impedance decreases more quickly at this frequency range. Otherwise, with the increasing loading of MWCNT, the impedance phase is independent of frequency in a wide frequency region, while the remarkable shift of impedance phase peak appears at high frequency [see rectangle frame with transverse lines in Fig. 1(a)]. In this case, the Ohmic resistance of the composites becomes strong and the capacitive reactance behavior is weak.

Figure 2 shows two half circles in the curves [here we show only an amplifactory half circle in inset of Fig. 2(a)], corresponding to the polarization at the middle frequency and high frequency, respectively. We think that the equivalent circuits of the MWCNT/RT-SR composites are basically composed of two parallel RC circuits in series, as shown in Fig. 2(e). In the applied circuits, the constant phase elements (CPEs) are used to simulate the impedance data instead of the ideal capacitor. For each RC unit, its complex impedance can be expressed as follows:¹⁷

$$Z^* = \frac{R}{(1 + j\omega CR)} = \frac{R}{1 + j\omega\tau}, \quad (1)$$

where $\tau = RC$ is the time constant of circuits. It is found from experiments there is no half circle occurring in the impedance spectra of RTV-SR matrix itself. It suggests that the electrical polarization of the MWCNT/RT-SR composites is concerned with the MWCNT. The R1 and CPE1 in the cir-

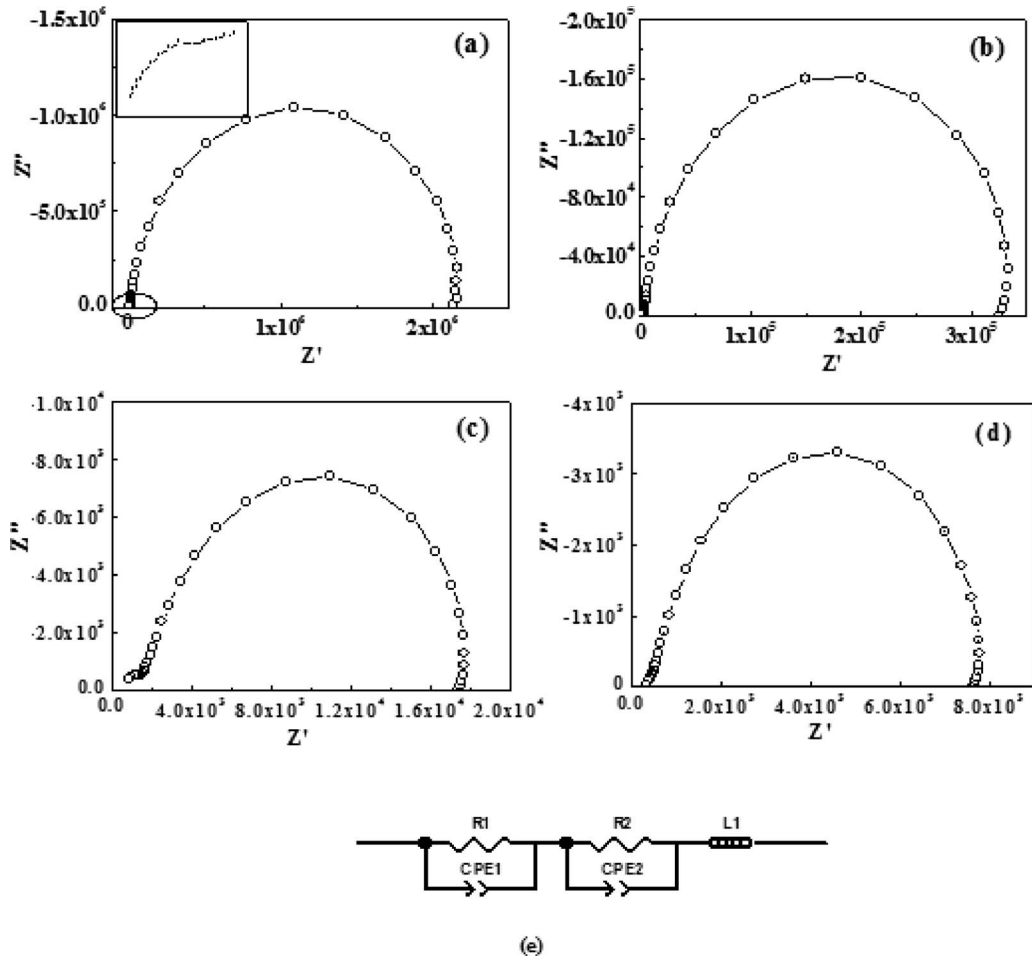


FIG. 2. Impedance spectra of the MWCNT/RT-SR composites at f_{MWCNT} =(a) 0.019, (b) 0.026, (c) 0.029, and (d) 0.032, respectively. (e) Equivalent circuits of the MWCNT/RT-SR composites.

circuits of Fig. 2(e) are produced by the polarization of the interfacial layer of MWCNT and RT-SR. However, the R2 and CPE2 represent the resistance and capacitance produced by the polarization of MWCNT at high frequency, respectively. The value of the time constant (in seconds) is equal to the product of the circuit resistance (in ohms) and the circuit capacitance (in farads), which is shown as follow:¹⁷

$$\omega_{max} = \tau^{-1} = (RC)^{-1}, \tag{2}$$

where ω_{max} is the frequency corresponding to the highest point of the half circle, that is, the frequency corresponding to the maximal Z'' . By using the ZVIEW2 software, the impedance data of sample can be simulated and the parameters of equivalent circuits are gained according to Eq. (1). The extracted parameters by fitting the impedance data to the equivalent circuits are shown in Table I. It is found that the resistances R1 and R2 decrease, while the CPE1 and CPE2 increase with the loading of MWCNT.

According to the equivalent circuits and Fig. 3(a), three distinct regions can be divided into the curve of dielectric permittivity versus frequency, such as low frequency region, middle frequency region, and high frequency region. In the low frequency region, the dielectric permittivity is huge and increases with MWCNT volume fraction f_{MWCNT} . Generally, at low frequency, the polarization time is long and the space

charge polarization plays a crucial role in the composites. As seen from Fig. 3(a), the dielectric permittivity of the MWCNT/RT-SR composite at $f_{MWCNT}=0.032$ is as high as 10^9 at 10^{-3} Hz. Furthermore, the dielectric permittivity decreases greatly with frequency, while the dielectric loss increases significantly with frequency in this region, which shows the space charge polarization character (response of charge carrier polarization). For the MWCNT/RT-SR composites, CNTs are conductive and silicone rubber is insulating so the space charge accumulates at the interface of composites and the charge is stored. With the increasing loading of MWCNT, more electrons supplied by CNTs contribute the

TABLE I. Extracted parameters from the circuit elements by fitting the impedance data to the equivalent circuits for different volume fractions of MWCNT f_{MWCNT} .

| Samples | R1 (Ω) | R2 (Ω) | CPE1 (F) | CPE2 (F) |
|-------------------|-------------------|--------|-----------------------|-----------------------|
| $f_{MWCNT}=0.019$ | 2.2×10^6 | 15 883 | 8.0×10^{-10} | 6.0×10^{-10} |
| $f_{MWCNT}=0.023$ | 1.6×10^6 | 12 348 | 6.7×10^{-10} | 2.1×10^{-9} |
| $f_{MWCNT}=0.026$ | 3.4×10^5 | 3 690 | 8.9×10^{-10} | 4.3×10^{-9} |
| $f_{MWCNT}=0.029$ | 16 041 | 2 346 | 1.5×10^{-9} | 3.1×10^{-7} |
| $f_{MWCNT}=0.032$ | 7 086 | 998 | 2.7×10^{-9} | 7.8×10^{-5} |

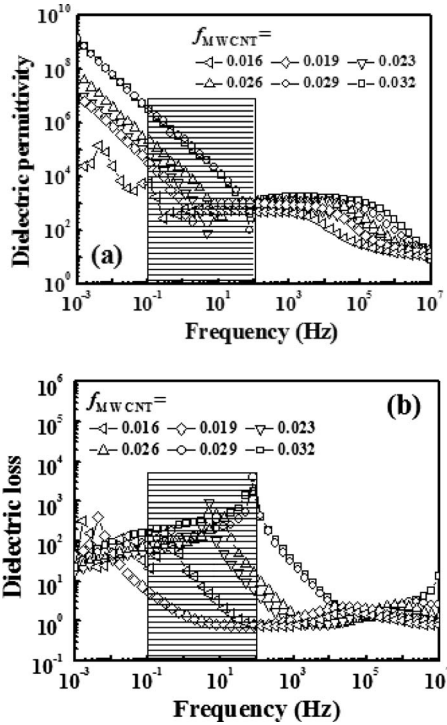


FIG. 3. Dependences of (a) dielectric permittivity and (b) dielectric loss of the MWCNT/RT-SR composites with different f_{MWCNT} on frequency from 10^{-3} to 10^7 Hz at RT.

remarkable space charge polarization. The dielectric permittivity versus frequency at this region can be described by the following expression:¹⁸

$$\epsilon_r = \omega^{n_{\text{LFD}}}, \quad (3)$$

where ϵ_r is the relative dielectric permittivity of composites, n_{LFD} is the exponent of low frequency dispersion (LFD), and $\omega = 2\pi\nu$ is the applied frequency. The remarkable behavior is known as LFD. The charge carriers are relatively free to move in the extended trajectories between the electrodes and therefore produce giant polarizabilities. This strong dispersion behavior is based on the hopping charge carrier, which dominates the conductance and dielectric response. The dispersion behavior becomes strong so that it spreads to high frequency with increasing f_{MWCNT} . The exponents n_{LFD} of the MWCNT/RT-SR composites at different f_{MWCNT} are shown in Table II.

Generally, the dielectric permittivity versus frequency curve is slippery and there are no peaks occurring. It is found from Fig. 3(a) that there is a sharp decreasing peak in the curves of dielectric permittivity versus frequency. As we know, all dielectrics have two types of losses. One is the conduction loss, representing the flow of actual charge through the dielectric. The other is a dielectric loss due to the motion/rotation of atoms or molecules in the ac field. According to the above analysis, the conduction of the

MWCNT/RT-SR composites is dominated by resistance at low frequency which produces a lot of conduction loss, the loss tangent is as high as 1000 [see Fig. 3(b)] and eventually produces a rise in temperature of the sample placed in the ac field. The high temperature causes the charge carriers moving in disorder and breaks slowly the regular arrangement of mobile charge carriers at the interface of composites. Therefore, a sharp peak appears in the dielectric permittivity spectrum.

In the middle frequency region, the polarization is mainly dependent on the localized hopping charge carriers at the interface layer response to the electric field, which produces the R1 and CPE1. The localized electrons of isolated CNTs hop which just like dipolar polarization and entitle the composites to store charge under the applied electric field. Meantime, two CNTs and the insulating polymer inside can be taken as a microcapacitor which entitles the composites to store charge. It is also found that the dielectric permittivity is less dependent on frequency until the relaxation happens and then the permittivity decreases quickly with frequency.

The relaxation time τ is often used when relaxation process is discussed, which represents the characteristic time of polarization relaxation. When the polarization of samples cannot follow the change in external electric field, the relaxation happens so that the corresponding dielectric permittivity decreases quickly and the dielectric loss increases. It is found that the relaxation frequency increases with the increase in f_{MWCNT} , as shown in Figs. 3(a) and 3(b). According to Eq. (3), the highest point of half circle of the ac impedance spectra responds to the relaxation frequencies. Therefore, the first and second relaxation frequencies (ν_1 and ν_2) can be gained, and the relaxation time is calculated, as shown in Table III. It can be noticed that the relaxation time decreases with the increasing loading of MWCNT. It is analyzed when the concentration of MWCNT increases, the interfacial potential energy decreases so that the localized charge carriers are easier to hop. As a result, the polarization is easy, which can adapt to the higher applied frequency. This induces the relaxation process at higher frequency.

Figure 4(a) shows the dependence of dielectric permittivity of the MWCNT/RT-SR composites at 10^3 Hz on the volume fraction of MWCNT. The dielectric permittivity increases with f_{MWCNT} . It is analyzed that the localized charge carriers must overcome certain potential barrier, jumps to another localized sites, and produces interfacial polarization. Therefore, the polymer layers become thinner gradually with the increasing loading of MWCNT. In this case, the potential energy decreases, which is helpful to the hopping of electrons. As a result, the conductivity and the dielectric permittivity increase both, as shown in Figs. 4(a) and 4(b). This is due to a simultaneous increase in the localized charges and the conductive paths. A further increase in the MWCNT loading yields to a continuous increase in the dielectric per-

TABLE II. Values of n_{LFD} calculated from Eq. (3) for the MWCNT/RT-SR composites at different concentrations.

| Samples | $f_{\text{MWCNT}}=0.019$ | $f_{\text{MWCNT}}=0.023$ | $f_{\text{MWCNT}}=0.026$ | $f_{\text{MWCNT}}=0.029$ | $f_{\text{MWCNT}}=0.032$ |
|------------------------|--------------------------|--------------------------|--------------------------|--------------------------|--------------------------|
| n_{LFD} value | -1.17 | -1.25 | -1.25 | -1.21 | -1.29 |

TABLE III. Relaxation time of the MWCNT/RT-SR composites at different f_{MWCNT} .

| | Sample | | | | |
|--------------|--------------------------|--------------------------|--------------------------|--------------------------|--------------------------|
| | $f_{\text{MWCNT}}=0.019$ | $f_{\text{MWCNT}}=0.023$ | $f_{\text{MWCNT}}=0.026$ | $f_{\text{MWCNT}}=0.029$ | $f_{\text{MWCNT}}=0.032$ |
| ν_1 (Hz) | 126 | 202 | 910 | 13 895 | 22 230 |
| τ_1 (s) | 0.0013 | 0.000 79 | 0.000 17 | 1.1×10^{-5} | 7.2×10^{-6} |
| ν_2 (Hz) | 59 6378 | 95 4127 | 2 811 860 | 3 907 054 | ... |
| τ_2 (s) | 2.7×10^{-7} | 1.7×10^{-7} | 5.7×10^{-8} | 4.1×10^{-8} | ... |

mittivity until the amount of MWCNTs is enough to connect most of the isolated conductive region together and most of the electrons give rise to direct current conduction. Otherwise, the increase in dielectric permittivity can also be explained by the fact that more microcapacitors are formed when the concentration of MWCNT increases, which allows high dielectric permittivity to the composites, as shown by the schematic image in the inset of Fig. 4(a). In the high

frequency region, the dielectric permittivity is mainly dependent on polarization of CNTs due to the function of space charge and the weakness of interfacial polarization.

As a special case, the dependence of conductivity of the MWCNT/RT-SR composite at $f_{\text{MWCNT}}=0.026$ on the frequency is shown in Fig. 4(c). The curve can be divided into three regions. In the first region, the conductivity is independent on frequency, and the value of conductivity corresponds to the dc conductivity. The equivalent circuits of the MWCNT/RT-SR composites are composed of parallel RC. As we know, a capacitor is equal to the open circuit state at low frequencies. As no charge flows through the insulating dielectric layer, so the conductivity is mainly dependent on the resistance. In this case, the conductivity of the composites does not change with the frequency. However, it is found from the inset in Fig. 4(c) that the $\log \sigma$ versus $\log \omega$ is in a good exponential relationship. The conductivity decreases with frequency weakly, and this indicates that the sample does not only behave as the pure resistance but also absorbs some electrons in this section which causes the LFD phenomenon. In the second region, the conductivity increases with frequency. The interfacial polarization of the MWCNT/RT-SR composites is induced, which also produces R1 and CPE1. In this region, the capacitor will only accumulate a limited amount of charge before the potential difference changes. The higher is the frequency, the less charge will be accumulated. The function of capacitor on ac conductivity stands out with an increase in frequency, both of the reactance and the parallel impedance decrease. On the other side, when the polarization relaxation happens, the accumulated charge moves with the applied electric field and produces the dc conductivity, which would improve the conductivity further. In the third region, the conductivity increases with frequency, and this region is responding to the polarization of CNTs. In short, at low frequencies, a frequency independent conductivity is recorded, which is attributed to resistive conduction through the bulk composite. On the other hand, at high frequencies, the conductivity appears to be proportional to frequency due to the capacitance of the host medium between the conducting particles or clusters.

Generally, the ac conductivity can be expressed as follows:¹⁸

$$\sigma(\omega) = \sigma_{\text{dc}} + A(\omega)^s, \quad (4)$$

where σ_{dc} is the dc conductivity at $\omega \rightarrow 0$, A and s parameters are dependent on temperature and the concentration of fillers.^{19,20} Equation (4) is often called the ac universal dielectric response since it has been found to satisfactorily de-

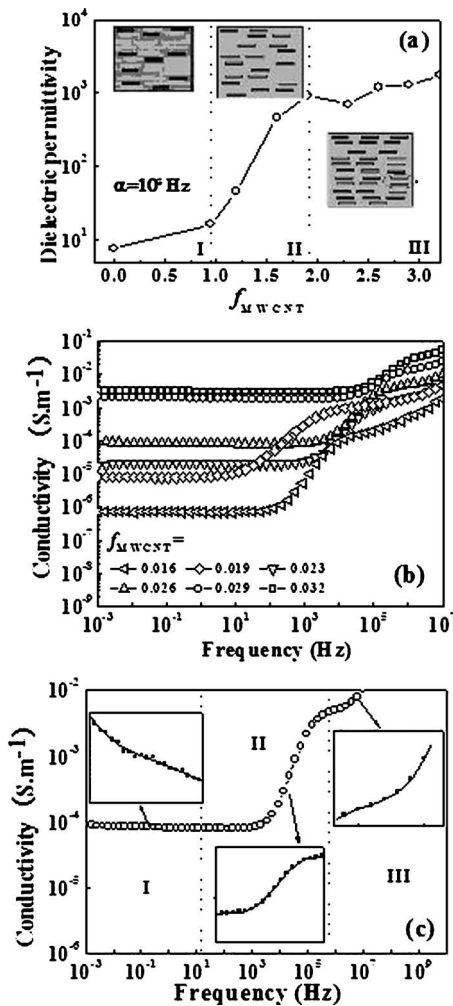


FIG. 4. (a) Dependence of dielectric permittivity on f_{MWCNT} in the MWCNT/RT-SR composites, measured at RT and 1 kHz; the insets show the formation process of microcapacitor networks with an increase in f_{MWCNT} . (b) Dependence of ac conductivity of the MWCNT/RT-SR composites with different f_{MWCNT} on frequency from 10^{-3} to 10^7 Hz at RT. (c) Dependence of ac conductivity of the MWCNT/RT-SR composites ($f_{\text{MWCNT}}=0.026$) on frequency from 10^{-3} to 10^7 Hz at RT, and the insets show the dependence of conductivity on frequency at (I) low, (II) middle, and (III) high frequency ranges, respectively.

scribe the ac response of numerous different types of materials, which can be classified as disordered solids.

IV. CONCLUSIONS

Based on the analysis of the ac impedance spectra, the equivalent circuits of MWCNT/RT-SR composites were built, and the law of polarization and the mechanism of electric conductance under the ac field were investigated. The results show that two parallel RC circuits in series are the equivalent circuits of the MWCNT/RT-SR composites. At low frequency, the conductivity is independent of the frequency. At middle and high frequencies, the conductivity increases with increasing frequency due to the effects of capacitance change and interfacial relaxation. The curve of dielectric permittivity versus frequency would be divided into three distinct regions. At low frequency, the polarization can be described by the LFD, which means it obeys basically the power law. At middle frequency, the dielectric permittivity is less dependent on frequency, which corresponds to the interfacial polarization of localized charges. At high frequency, the polarization is dependent on the CNTs. The dielectric permittivity of the MWCNT/RT-SR composites is mainly relative to the quantity of the localized charges and the interfacial potential energy. It is found both conductivity and dielectric permittivity increase with the increase in the MWCNT loading because the potential energy decreases. However, after most of the CNTs take part in the conductive networks, the dielectric permittivity of composites decreases.

ACKNOWLEDGMENTS

This work was financially supported by NSF of China (Grant No. 50677002), NSF of Beijing City (Grant No. 2083031), the Ministry of Sciences and Technology of China

through 863-Project (Grant No. 2008AA03Z307), Program for Changjiang Scholars and Innovative Research Team in University (PCSIRT Grant No. IRT0807), Program for New Century Excellent Talents in University (NCET).

- ¹Q. M. Zhang, H. F. Li, M. Poh, F. Xia, Z. Y. Cheng, H. S. Xu, and C. Huang, *Nature (London)* **419**, 285 (2002).
- ²Y. Li, *Phys. Rev. Lett.* **90**, 217601 (2003).
- ³Z. M. Dang, L. Wang, Y. Yin, Q. Zhang, and Q. Q. Lei, *Adv. Mater. (Weinheim, Ger.)* **19**, 852 (2007).
- ⁴V. Bohner, A. Levstik, C. Huang, and Q. M. Zhang, *Phys. Rev. Lett.* **92**, 047604 (2004).
- ⁵C. Ang and Z. Yu, *Adv. Mater. (Weinheim, Ger.)* **16**, 979 (2004).
- ⁶Y. Shen, Y. Lin, M. Li, and C. W. Nan, *Adv. Mater. (Weinheim, Ger.)* **19**, 1418 (2007).
- ⁷B. J. Landi, R. P. Raffaele, M. J. Heben, J. L. Alleman, W. VanDerveer, and T. Gennett, *Nano Lett.* **2**, 1329 (2002).
- ⁸L. Qi, B. I. Lee, S. Chen, W. D. Samuels, and G. J. Exarhos, *Adv. Mater. (Weinheim, Ger.)* **17**, 1777 (2005).
- ⁹J. Li, S. I. Seok, B. Chu, F. Dogan, Q. M. Zhang, and Q. Wang, *Adv. Mater. (Weinheim, Ger.)* **21**, 217 (2009).
- ¹⁰C. Y. Chiu, H. W. Chen, S. W. Kuo, C. F. Huang, and F. C. Chang, *Macromolecules* **37**, 8424 (2004).
- ¹¹C. J. Dias and D. K. Das-Gupta, *IEEE Trans. Dielectr. Electr. Insul.* **3**, 706 (1996).
- ¹²T. A. Ezquerra, M. T. Connor, S. Roy, M. Kuleszka, J. Fernandes-Nascimento, and F. J. Balta-Celleja, *Compos. Sci. Technol.* **61**, 903 (2002).
- ¹³J. C. Dyre, *J. Appl. Phys.* **64**, 2456 (1988).
- ¹⁴J. C. Dyre and T. B. Schröder, *Rev. Mod. Phys.* **72**, 873 (2000).
- ¹⁵A. R. Hippel, *Dielectrics and Waves* (Artech House, Boston, 1995).
- ¹⁶S. Zhang, N. Zhang, C. Huang, K. Ren, and Q. M. Zhang, *Adv. Mater. (Weinheim, Ger.)* **17**, 1897 (2005).
- ¹⁷C. W. Nan, *Prog. Mater. Sci.* **37**, 1 (1993).
- ¹⁸A. K. Jonscher, *Universal Relaxation Law* (Chelsea Dielectric, London, 1992).
- ¹⁹G. M. Tsangaris, G. C. Psarras, and E. Manolakaki, *Adv. Compos. Lett.* **8**, 25 (1999).
- ²⁰R. R. Vijayalakshmi and M. H. Shridhar, *Mater. Lett.* **55**, 34 (2002).